сообщения
объединенного
института
ядерных
исследований
дубна

E1-89-481

C.Damdinsuren, V,I,Ilyushchenko, P.Kozma,
D.Chultem *

YIELDS OF RADIONUCLIDES FORMED IN THE INTERACTION OF 3.65 AGeV ^{12}C-IONS AND PROTONS WITH ^{nat}Pb

---

*Mongolian State University, Ulan Bathor

1989

Дамдинсурэн Ц. и др. E1-89-481

Выходы радиоактивных ядер, образующихся при взаимодействии ядер ^{12}C и протонов с ^{nat}Pb при энергии 3,65 АГэВ

На дубненском синхрофазотроне исследованы процессы образования радиоактивных ядер в реакциях ^{12}C и протонов с ^{nat}Pb при энергии 3,65 АГэВ. Независимые и кумулятивные выходы фрагментов мишени определены по методу γ-спектроскопии. Из полученных данных найдены изомерные отношения и массовые распределения.

Работа выполнена в Лаборатории высоких энергий ОИЯИ.

Сообщение Объединенного института ядерных исследований. Дубна 1989

Damdinsuren C. et al. E1-89-481

Yields of Radionuclides Formed in the Interaction of 3.65 AGeV ^{12}C-Ions and Protons with ^{nat}Pb

The production of radionuclides in the reactions of 3.65 AGeV ^{12}C-ions and protons with ^{nat}Pb has been investigated at the Dubna synchrophasotron. The independent and cumulative yields of target residues were determined by off-line gamma-ray spectroscopy. Isomeric ratios and mass-yield distributions were deduced from these data.

The investigation has been performed at the Laboratory of High Energies, JINR.

Communication of the Joint Institute for Nuclear Research. Dubna 1989

1. Introduction

In recent years great interest has been shown in experimental studies of relativistic heavy-ion /RHI/ reactions, prompted partly by the possibilities of studying nuclear matter at high densities and behaviour of emitted fragments, verifying various reaction models and fundamental hypotheses of high-energy physics, as well. In RHI reactions with heavy target nuclei a large number of created residues forms a good statistical basis for obtaining their mass-yield distributions.

In this paper, we report the results of radioanalytical measurements of the yields of the target residues formed in the reactions of 3.65 AGeV ^{12}C-ions and 3.65 GeV protons with a natural Pb target. The purpose of this investigation is to see if the target-residue mass distributions show any unusual features that could help us to understand the mechanism of reactions at high energies. Moreover, the availability to accelerate at the Dubna synchrophasotron RHI and protons of the same AGeV energy could give us the possibility to compare mass-yield distributions in both reactions.

2. Experimental procedure

The target stacks for this experiment consisted of three foils from natural lead. The outer foils were used for recoil loss compensation, the middle one was analysed. The target foils, varying in thickness from 45 to 120 mg/cm^2 and surrounded by $\sim$175 mg/cm^2 Mylar catcher foils, were irradiated with ^{12}C-ions and protons in an external beam of the Dubna synchrophasotron. Irradiation periods were chosen to achieve $\sim 10^{13}$ total flux particles in both experiments.

Gamma-ray spectroscopic measuremnts of the radioactivity induced in the target foils began one hour after irradiations lasting for about three weeks. The spectra were analysed with computer programs which subtracted the background under the peaks and fitted the Gaussian peaks to the data points. Radionuclides were identified on the basis of their gamma-ray energies, half-lives and fractional abundances taken from the Gamma-Ray Catalogue /1/. Pertinent characteristics of radionuclides carefully identified in both investigations are displayed in Table 1. In this table symbols I, C$^+$ and C$^-$ are used for independent, neutron-deficient and neutron excessive cumulative yields, respectively.

Table 1. Decay properties of observed radionuclides:

Nuclide	Type of yield	Energy /keV/	Fractional abundance /%/	Half-life /h=hours,d=days/
$^{24}\mathrm{Na}$	C^-	1369	100.0	15.02 h
$^{28}\mathrm{Mg}$	C^-	1779	100.0	20.90 h
$^{41}\mathrm{Ar}$	C^-	1294	99.1	1.83 h
$^{43}\mathrm{K}$	C^-	373	87.9	22.30 h
$^{44}\mathrm{Sc}^{m}$	I	271 1157	77.8 100.0	2.44 d
$^{46}\mathrm{Sc}$	I	1121	100.0	83.83 d
$^{48}\mathrm{Sc}$	I	984	100.0	43.70 h
$^{54}\mathrm{Mn}$	I	835	100.0	312.5 d
$^{57}\mathrm{Ni}$	I	1378	77.9	36.10 h
$^{59}\mathrm{Fe}$	C^-	1292	43.2	44.5 d
$^{72}\mathrm{As}$	I	834	79.5	26.00 h
$^{73}\mathrm{Se}$	C^+	361	97.0	7.15 h
$^{76}\mathrm{Br}$	I	559 657	72.3 15.5	16.20 h
$^{77}\mathrm{Br}$	C^+	239	23.9	2.38 d
$^{81}\mathrm{Rb}$	C^+	190 446	64.3 23.3	4.58 h
$^{82}\mathrm{Rb}^{m}$	I	554 777	62.8 84.5	6.47 h
$^{84}\mathrm{Rb}$	I	882	67.8	32.87 d
$^{86}\mathrm{Y}$	I	1077 1153	82.5 30.5	14.74 h
$^{86}\mathrm{Zr}$	C^+	243	95.8	16.50 h
$^{87}\mathrm{Y}^{m}$	C^+	381	78.1	12.90 h
$^{90}\mathrm{Nb}$	I	141 1129	69.0 92.0	14.60 h
$^{92}\mathrm{Sr}$	C^-	1384	90.0	2.71 h
$^{93}\mathrm{Mo}^{m}$	I	685	99.7	6.85 h
$^{93}\mathrm{Tc}$	C^+	1363	65.8	2.75 h

Table 1 /continued/

Nuclide	Type of yield	Energy /keV/	Fractional abundance /%/	Half-life /h=hours,d=days/
$^{94}\mathrm{Tc}$	I	703 850 871	99.8 97.7 100.0	4.88 h
$^{95}\mathrm{Tc}$	C^+	766	93.9	20.00 h
$^{96}\mathrm{Nb}$	I	778	96.9	23.35 h
$^{96}\mathrm{Tc}$	I	778 850	100.0 97.8	4.28 d
$^{99}\mathrm{Mo}$	C^-	140	90.7	2.75 d
$^{103}\mathrm{Ru}$	C^-	497	89.5	39.25 d
$^{111}\mathrm{In}$	C^+	171 245	90.3 94.0	2.83 d
$^{112}\mathrm{Pd}$	C^-	617	50.0	21.05 h
$^{119}\mathrm{Te}$	C^+	644	84.5	16.05 h
$^{119}\mathrm{Te}^{m}$	C^+	1213	66.7	4.69 d
$^{121}\mathrm{Te}$	C^+	573	80.3	16.80 d
$^{121}\mathrm{Te}^{m}$	C^+	212 573	81.4 80.3	154.0 d
$^{121}\mathrm{I}$	C^+	212	85.0	2.12 h
$^{122}\mathrm{Sb}$	I	564	70.0	2.70 d
$^{123}\mathrm{Te}^{m}$	I	159	84.0	119.7 d
$^{123}\mathrm{I}$	C^+	159	83.3	13.20 h
$^{124}\mathrm{Sb}$	I	603 1691	98.4 49.0	60.2 d
$^{125}\mathrm{Xe}$	C^+	188 243	54.9 28.8	16.90 h
$^{127}\mathrm{Xe}$	C^+	172 203	25.5 68.3	36.41 d
$^{127}\mathrm{Cs}$	C^+	412	58.4	6.25 h
$^{128}\mathrm{Ba}$	C^+	443	25.8	2.43 d
$^{131}\mathrm{Ba}$	C^+	496	47.1	11.5 d
$^{131}\mathrm{Te}^{m}$	C^-	774	38.1	30.00 h
$^{132}\mathrm{La}$	C^+	465	77.0	4.80 h

Table 1 /continued/

Nuclide	Type of yield	Energy /keV/	Fractional abundance /%/	Half-life /h=hours,d=days/
^{132}Ce	C^+	183	79.0	3.51 h
^{135}Ce	C^+	266	42.4	17.60 h
^{145}Eu	C^+	894	65.8	5.94 d
^{139}Nd^{m}	C^+	114	34.0	5.50 h
^{147}Gd	C^+	229	64.4	38.10 h
^{149}Gd	C^+	150	41.7	9.4 d
^{149}Tb	C^+	165	26.6	4.15 h
^{151}Tb	C^+	252	26.0	17.60 h
^{152}Tb	C^+	344	57.0	17.50 h
^{155}Dy	C^+	227	68.8	10.00 h
^{157}Dy	C^+	326	93.2	8.10 h
^{158}Er	C^+	218	43.0	2.25 h
^{161}Er	C^+	827	61.5	3.24 h
^{166}Yb	C^+	184 779	21.3 24.9	2.36 d
^{169}Yb	C^+	177 198	22.0 36.0	32.02 d
^{170}Hf	C^+	165 621	33.5 22.9	16.00 h
^{171}Hf	C^+	662	14.8	12.10 h
^{171}Er	C^-	308	64.4	7.52 h
^{173}Hf	C^+	124 297	82.7 33.8	23.90 h
^{175}Hf	C^+	343	86.6	70.00 d
^{175}Ta	C^+	207	13.3	10.50 h
^{176}Ta	C^+	1159	23.8	8.08 h
^{177}W	C^+	116	58.5	2.25 h
^{181}Re	C^+	366	56.4	20.00 h
^{182}Re	C^+	229 1121	27.9 23.9	2.67 d

Table 1 /continued/

Nuclide	Type of yield	Energy /keV/	Fractional abundance /%/	Half-life /h=hours,d=days/
^{182}Os	C^+	180 510	36.8 55.0	21.60 h
^{183}Os^{m}	C^+	1102	50.0	9.90 h
^{184}Re	C^+	792	77.4	38.0 d
^{184}Ir	C^+	120 264 390	30.3 67.5 25.7	3.02 h
^{186}Ir	C^+	137 297 435	41.3 62.2 33.8	15.80 h
^{186}Ir^{m}	C^+	137	30.5	1.75 h
^{186}Pt	C^+	689	100.0	2.00 h
^{190}Re^{m}	C^-	187	50.5	3.30 h
^{192}Hg	C^-	275	45.0	4.90 h
^{192}Au	C^+	317	78.3	5.03 h
^{193}Hg^{m}	C^+	258 408	58.0 37.0	11.80 h
^{196}Tl	C^+	426	83.7	1.84 h
^{196}Tl^{m}	C^+	426 695	91.0 41.0	1.41 h
^{197}Hg^{m}	C^+	134	34.1	23.80 h
^{198}Tl	C^+	412	81.8	5.30 h
^{198}Tl^{m}	I	587 637	51.0 55.0	1.87 h
^{198}Pb	C^+	173 290	18.0 36.0	2.40 h
^{198}Au	C^-	412	95.5	2.70 d
^{199}Tl	C^+	208 247	12.2 9.2	7.42 h
^{200}Au^{m}	C^-	579	72.0	18.70 h
^{200}Tl	C^+	368	87.2	26.10 h
^{200}Pb	C^+	148	37.7	21.50 h
^{201}Tl	C^+	167	10.6	3.04 d

Table 1 /continued/

Nuclide	Type of yield	Energy /keV/	Fractional abundance /%/	Half-life /h=hours,d=days/
^{201}Pb	C^{+}	331	78.7	9.33 h
^{202}Tl	C^{+}	440	91.4	12.23 h
^{202}Pb^{m}	C^{+}	422 658 787 961	85.5 32.3 49.7 91.4	3.53 h
^{202}Bi	C^{+}	658 961	60.6 99.3	1.72 h
^{203}Hg	C^{-}	279	81.5	46.58 d
^{203}Pb	C^{+}	279	80.1	2.16 d
^{203}Bi	C^{+}	820	29.6	11.76 h
^{204}Bi	C^{+}	375 899 984	81.0 98.5 58.0	11.22 d
^{204}Po	C^{+}	884	30.3	3.53 h
^{206}Bi	C^{+}	803	98.9	6.24 d
^{206}Po	C^{+}	511 807	24.4 23.0	8.80 d
^{207}Bi	C^{+}	570 1064	97.8 74.9	33.40 y

3.Results

The experimentally determined independent and cumulative yields for individual radionuclides from the p+^{nat}Pb and ^{12}C+^{nat}Pb reactions at 3.65 AGeV are listed in Table 2. They are related to the cross sections of the ^{27}Al(p,X)^{24}Na and ^{27}Al(^{12}C,X)^{24}Na monitoring reactions /2/. For a radionuclide emitting more than one assayed gamma-ray /see Table 1/, the weighted average yield is reported. The errors assigned to the yields are based on our estimates of errors from the counting statistics, detector efficiencies and target thickness. A systematic error of about 10% corresponding to the beam flux monitor is not included in the tabulated values.

Table 2. Yields for the production of radionuclides in the interaction of lead with 3.65 AGeV ^{12}C-ions and 3.65 GeV protons:

Nuclide	Y(^{12}C)	Y(p)	Nuclide	Y(^{12}C)	Y(p)
^{24}Na	40.5±8.7	15.9±1.4	^{111}In	19.1±2.6	8.1±0.7
^{28}Mg	7.2±2.0	2.8±0.2	^{112}Pd		14.8±1.9
^{41}Ar		0.7±0.1	^{119}Te	15.0±3.8	6.7±1.4
^{43}K	3.3±1.0		^{119}Te^{m}	1.5±0.3	0.8±0.1
^{44}Sc^{m}		1.2±0.2	^{121}Te	20.2±2.7	8.9±0.8
^{46}Sc	13.2±1.1	5.9±0.6	^{121}Te^{m}	1.9±0.3	0.7±0.1
^{48}Sc	2.5±0.4	1.0±0.1	^{121}I	9.0±1.9	4.7±0.6
^{54}Mn	8.5±1.7	3.3±0.3	^{122}Sb	10.5±2.4	4.6±0.7
^{57}Ni	4.1±1.3		^{123}Te^{m}	8.7±1.9	
^{59}Fe	3.5±0.6	1.7±0.2	^{123}I	12.1±3.3	5.4±0.7
^{72}As	6.4±1.3	3.4±0.8	^{124}Sb	15.9±3.7	6.5±0.6
^{73}Se	3.5±1.7		^{125}Xe	8.1±0.9	
^{76}Br	2.0±1.4		^{127}Xe	27.2±5.8	10.0±1.1
^{77}Br	3.6±0.8	1.6±0.3	^{127}Cs		11.2±1.4
^{81}Rb	13.6±1.9	5.5±0.6	^{128}Ba	10.0±2.4	3.8±0.9
^{82}Rb^{m}	6.5±0.8		^{131}Ba	19.7±5.6	10.4±1.0
^{84}Rb	6.0±1.2	1.7±0.3	^{131}Te^{m}	8.3±1.4	
^{86}Y	7.2±1.9	3.9±0.8	^{132}La		4.0±0.6
^{86}Zr	5.7±1.0		^{132}Ce	6.2±0.9	4.0±0.7
^{87}Y^{m}	8.7±1.1		^{135}Ce	12.9±1.4	
^{90}Nb		3.3±0.4	^{139}Nd^{m}	9.3±1.7	
^{92}Sr	3.9±1.2		^{145}Eu	20.0±5.1	9.4±1.0
^{93}Mo^{m}	2.5±0.7	1.4±0.3	^{147}Gd	12.4±2.7	6.5±0.9
^{93}Tc	3.3±0.5	1.5±0.2	^{149}Gd	21.4±5.7	15.0±1.3
^{94}Tc		2.8±0.4	^{149}Tb	12.7±1.8	
^{95}Tc	9.0±1.1		^{151}Tb	16.6±2.9	16.4±4.9
^{96}Nb	5.5±1.3		^{152}Tb	18.5±4.0	6.7±1.2
^{96}Tc	2.8±0.7	1.1±0.3	^{155}Dy	12.8±1.4	
^{99}Mo		1.8±0.3	^{157}Dy	30.0±3.1	13.1±1.7
^{103}Ru	1.6±0.4	0.5±0.1	^{158}Er		15.0±6.5
^{161}Er	32.5±4.4		^{196}Tl	30.2±6.9	14.2±2.5
^{166}Yb	19.3±4.0		^{196}Tl^{m}	18.7±4.0	7.5±1.2
^{169}Yb	37.5±9.2	15.0±1.9	^{197}Hg^{m}		4.7±2.5
^{170}Hf	29.1±4.8		^{198}Tl	45.0±10	22.6±4.6
^{171}Hf	15.5±2.6		^{198}Tl^{m}	21.4±5.2	11.3±3.7
^{171}Er		11.0±3.7	^{198}Pb	52±10	
^{173}Hf	33.0±8.5	15.9±2.7	^{198}Au	38±8	

Table 2 /continued/

Nuclide	Y(^{12}C)	Y(p)	Nuclide	Y(^{12}C)	Y(p)
^{175}Hf		17.7±1.9	^{199}Tl		25±7
^{175}Ta	19.2±3.1		^{200}Au^{m}	31±12	
^{176}Ta	28.0±3.5		^{200}Tl	44±17	
^{177}W		15.0±3.3	^{200}Pb	70±13	62±12
^{181}Re	35.5±7.7		^{201}Tl	56±12	
^{182}Re	28.6±6.9		^{201}Pb	75±19	38±7
^{182}Os	33.2±4.5	16.9±1.8	^{202}Tl		15±3
^{183}Os^{m}		13.8±1.6	^{202}Pb^{m}	45±10	20±3.5
^{184}Re	15.0±8.7		^{202}Bi	33±8	
^{184}Ir	24.5±7.0		^{203}Pb		32±8
^{186}Ir	20.9±6.8		^{203}Bi	78±17	35±7
^{186}Pt	37.1±8.0		^{204}Bi	63±12	
^{190}Re^{m}	48.2±11.6		^{204}Po	39±7	
^{192}Hg		23.3±8.6	^{206}Bi	47±10	
^{192}Au	52±10	36±6	^{206}Po	68±15	
^{193}Hg^{m}	45±17		^{207}Bi	50±12	

Using the procedure previously described in detail /3/, the measured cumulative yields for precursory β-decay were iteratively corrected, the Gaussian charge-dispersion of the form

$$Y(A,Z)=(2\pi\sigma^2)^{1/2}\exp\{-(Z-Z_p(A))^2/2\sigma^2\}$$

were fitted to these data /4/, and the charge dispersions were integrated to give the isobaric yields for the reactions. The obtained mass-yield distributions of target residues are shown in Fig.1. The points are the experimental isobaric yields for the p+^{nat}Pb and ^{12}C+^{nat}Pb reactions, respectively, the appropriate curves being guides to the eye. As is seen, the p+^{nat}Pb and ^{12}C+^{nat}Pb mass-yield distributions display common features. The similarity between the mass-yield distributions of the target residues from the reactions of ^{nat}Pb with RHI and protons of the same AGeV energy may be viewed as an evidence for the factorization in these reactions /5/.

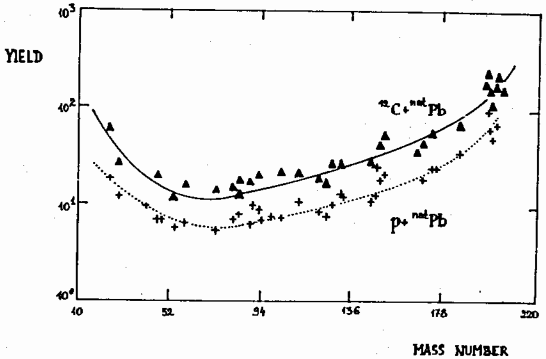

Fig.1. Mass-yield distributions of target residues from the reactions of 3.65 AGeV ^{12}C-ions and protons with ^{nat}Pb.

Table 3. Isomeric ratios

Isomeric ratio \ Reaction	^{12}C + ^{nat}Pb	p + ^{nat}Pb
$\frac{Y(^{119}Te^{m}\ (11/2^{-}))}{Y(^{119}Te\ \ (1/2^{+}))}$	0.10±0.05	0.12±0.04
$\frac{Y(^{121}Te^{m}\ (11/2-))}{Y(^{121}Te\ \ (1/2^{+}))}$	0.09±0.03	0.08±0.02
$\frac{Y(^{196}Tl^{m}\ (7^{+}))}{Y(^{196}Tl\ \ (2^{-}))}$	0.62±0.30	0.53±0.19
$\frac{Y(^{198}Tl^{m}\ (7^{+}))}{Y(^{198}Tl\ \ (2^{-}))}$	0.48±0.24	0.50±0.25

Table 3 shows isomeric ratios obtained in the reactions under study. It is seen that light spin member of an isomeric pair implies either low initial product angular momentum and/or removal of large amount of angular momenta by photon and/or particle emission during the de-excitation process /6/.

The cooperation of Prof. Ts.Vylov, Prof. K.D.Tolstov and Drs. V.B.Brudanin, A.Duka-Zolyómi, Sh.Gerbish, J.Kliman and the staff of the Dubna synchrophasotron is gratefully acknowledged.

REFERENCES

1. U.Reus, W.Westmeier, Atomic and Nuclear Data Tables 29 /1983/ 1-493.
2. C.Damdinsuren, V.M.Dyachenko, A.Duka-Zolyómi, J.Kliman, P.Kozma, B.Tumendemberel, Report JINR P1-87-932, Dubna, 1987.
3. C.Damdinsuren, P.Kozma, B.Tumendemberel, R.Khorolyjav, D.Chultem, Report JINR P1-88-135, Dubna, 1988.
4. P.Kozma, J.Kliman, M.Leonard, Czech.J.Phys. B 38 /1988/ 973.
5. R.P.Feynman, Phys.Rev.Lett. 23 /1969/ 1415.
6. W.Loveland, R.J.Otto, D.J.Morrissey, G.T.Seaborg, Phys.Lett. B 69 /1977/ 284.

Received by Publishing Department
on June 26, 1989.